J Solid State Electrochem (2007) 11:1405–1410
DOI 10.1007/s10008-007-0371-8

ORIGINAL PAPER

Investigation on cell impedance for high-power lithium-ion batteries

Dae-Keun Kang · Heon-Cheol Shin

Received: 2 January 2007 / Revised: 7 March 2007 / Accepted: 5 June 2007 / Published online: 3 July 2007

Abstract Variation of the dc polarization with time has been successfully calculated semiempirically for the lithium-ion battery at a variety of discharging rates. In particular, with the help of circuit analysis, the contribution of the uncompensated ohmic resistance, interfacial impedance, and diffusion impedance to total cathodic polarization has been satisfactorily differentiated as a function of discharging time. In the present work, a simple and practical method has been suggested to help one design effectively the high-power lithium-ion batteries.

Keywords High-power battery · Hybrid electric vehicle · Cell design · Cell resistance · Current pulse

Introduction

Much attention has been recently paid to high-power energy conversion devices for the application of transportation systems such as electric motors, hybrid electric vehicle, ship, aircraft, etc., mainly because of the exhaustion of fossil fuel and the environmental issues [1–3]. The key to successful development of a high-power battery system is to find the optimum design of the cell to minimize the polarization during the operation. This implies all the elements that affect the cell polarization should be seriously considered for the high-power cell design, unlike the high-capacity cell design where the intrinsic-specific capacity of the active materials and the effective use of the space inside the battery can are the critical issues, apart from the safety problems [4].

In this communication, we suggest the useful guideline to analyze the dc polarization of the lithium-ion battery. This fast and reliable method includes the differentiation of the elementary polarization caused by uncompensated ohmic resistance, interfacial impedance, and diffusion impedance with the help of the circuit analysis, based on the results of electrochemical impedance spectroscopy. Critical factors to affect the power performance of the cell were also discussed using the concept of fractional contribution of the cell elements to total dc polarization.

Dedicated to Professor Su-II Pyun on the occasion of his 65th birthday.

D.-K. Kang · H.-C. Shin (✉)
School of Materials Science and Engineering,
Pusan National University,
San30, Jangjeon-dong, Keumjung-ku,
Busan 609-735, South Korea
e-mail: hcshin@pusan.ac.kr

Materials and methods

A two-electrode electrochemical cell (Hohsen) was employed for electrochemical measurements using lithium foil as the counter and reference electrode. The working electrode was composed of 90 wt% $LiCoO_2$ (Aldrich), 5 wt% carbon black, and 5 wt% polyvinylidene fluoride binder in *n*-methyl pyrrolidinone. The slurry mixture was cast on Al foil, followed by drying at 150 °C in vacuum for 12 h, and uniaxial pressing between two flat plates at 500 psi for 5 min. A Celgard 2400 separator, wetted with 1 M solution of $LiPF_6$ in a 50/50 (v/v) mixture of ethylene carbonate (EC) and diethyl carbonate (DEC), was sandwiched between a $LiCoO_2$ working electrode and a lithium counter electrode. All cells were assembled and tested in a glove box (Vacuum Atmospheres Company) filled with purified argon gas. A Solartron 1287 electrochemical interface was employed to carry out the galvanostatic charge/discharge cycling and current pulse test. For the electrochemical

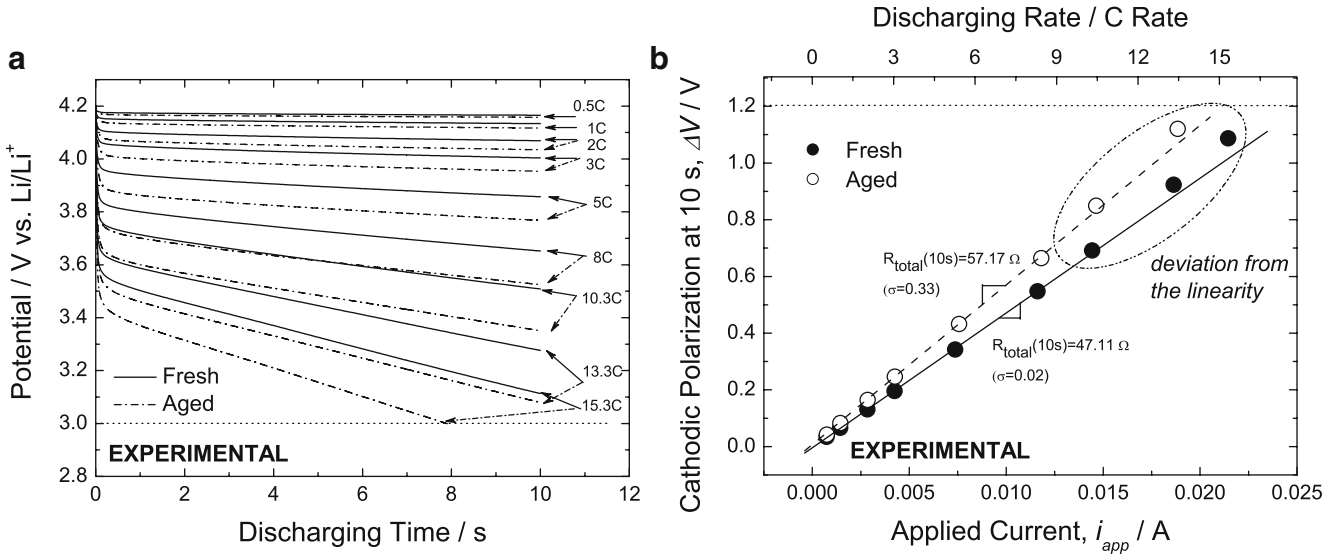

Fig. 1 **a** Experimental potential transients obtained from the fresh (*solid line*) and aged cell (*dotted line*) during the 10-s current pulse at a variety of discharging rates and **b** the variation of cathodic polarization at 10 s with applied current, reproduced from **a**

impedance measurements, the Solartron 1287 electrochemical interface was coupled with the Solartron 1455A frequency response analyzer.

The as-prepared cell was first cycled five times between 3.0 and 4.2 V (vs Li/Li^+) at the charge/discharge rate of 0.2*C* (this is called "fresh cell" hereafter). After the impedance measurement and the current pulse test, the cell was cycled 20 times under the same conditions as the as-prepared cell was initially cycled (this is called "aged cell" hereafter). The capacity retention of the aged cell was approx. 80%, as compared with the capacity of the fresh cell. Furthermore, finally, the impedance measurement and the current pulse test were carried out for the aged cell.

For the current pulse test, a constant voltage of 4.2 V (vs Li/Li^+) was first applied to the electrode for 2 h in order for the electrode to be equilibrated at that potential. Subsequently, discharging currents in the range of 0.74 (*C*/2 rate: a nominal specific capacity of 120 mAh g^{-1} was assumed to convert the current density into *C* rate) to 22.6 mA cm^{-2} (15.3*C*) were applied until either the electrode potential reached the lower cutoff voltage of 3.0 V (vs Li/Li^+) or the electrode is discharged for 10 s at the potential above 3.0 V (vs Li/Li^+). For the electrochemical impedance measurements, the electrode was maintained at the constant potential of 4.2 V (vs Li/Li^+) for 2 h. Then, the impedance measurements were carried out by applying an ac amplitude of 5 mV_{rms} on an equilibrium potential of 4.2 V (vs Li/Li^+) over the frequency range of 10 mHz to 100 kHz.

Results and discussion

Shown in Fig. 1 are the typical potential transients during the 10-s square current pulse at a variety of discharging (lithium insertion) rates of *C*/2 (0.74 mA cm^{-2}) to 15.3*C* (22.6 mA cm^{-2}). All the transients show an abrupt drop at the moment of the application of the current, followed by a gentle decrease in potential with time. The rate of potential change is getting higher with increasing discharging rate. It is noted that for the fresh cell (solid line), cell potential remains above the lower cutoff voltage of 3.0 V (vs Li/Li^+) throughout the whole discharging process even at the very high rate of 15.3*C*. On the contrary, cell potential falls below 3.0 V (vs Li/Li^+) at approx. 8 s for the aged cell

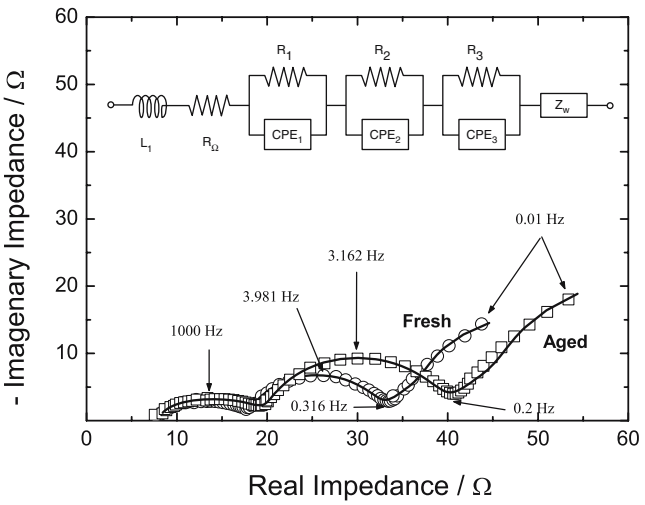

Fig. 2 Typical impedance spectra for the fresh (*open circle*) and aged cells (*open square*) with a configuration of Li|1 M $LiPF_6$-EC/DEC|$LiCoO_2$, measured at an electrode potential of 4.2 V (vs Li/Li^+). The *inset* is the equivalent circuit used for the analysis of discharging process of $LiCoO_2$, where *CPE* and Z_W are the constant phase element because of the capacitance dispersion and solid-state diffusion (or Warburg) impedance, respectively. *Solid lines* were determined from the CNLS fitting methods of the impedance spectra to the equivalent circuit

Table 1 Parameters determined from the CNLS fitting of impedance spectra (Fig. 2) to the equivalent circuit (inset of Fig. 2)

	L_1 (H)	R_Ω (Ω)	R_1 (Ω)	CPE_1 (F)		R_2 (Ω)	CPE_2 (F)		R_3 (Ω)	CPE_3 (F)		σ^b in Z_W
				C^a	η^a		C^a	η^a		C^a	η^a	
Fresh	2.42 μm	6.68	2.72	0.79 m	0.76	9.08	0.16 m	0.63	12.2	2.79 m	0.98	4.32
Aged	1.79 μm	6.90	3.00	0.79 m	0.79	10.23	0.17 m	0.63	17.0	2.80 m	0.98	4.89

[a] Constant phase element (CPE) was expressed in the form of $C(j\omega)^{\eta}$
[b] σ is the Warburg coefficient defined as $Z_W = \sigma\omega^{-0.5}(1-j)$, where ω is the angular frequency.

(dotted line) at the same discharging rate, implying that the aged cell has the higher cell resistance as compared with the fresh cell. In other words, practically one can draw continuously the charge for 10 s at the rate of 15.3*C* from the fresh cell, whereas one can make the aged cell continuously discharged at most for 8 s at the same rate.

To further investigate the potential drop at 10 s, the change in the cathodic polarization with the discharging rate (Fig. 1b) was reproduced from Fig. 1a. Apparent total cell resistance at 10 s was estimated, from the linear relationship between polarization (ΔV) and applied current (i_{app}), to be 45.11 and 57.17 Ω for the fresh cell and the aged cell, respectively, at the discharging rate less than 10*C*. The i_{app}–ΔV relation starts to deviate from the linearity at the rate above 10*C*. This indicates that there is additional increase in the polarization at the very high current drain. One of the possible reasons for the additional polarization is the limiting current behavior of the lithium ion transport through the pores of the separator wetted with the electrolyte [5]. Nevertheless, the origin of this phenomenon is still open to discussion.

The key to develop the high-power battery is up to how we can significantly reduce the polarization or how we can increase the maximum discharging rate where the cell potential remains above the lower cutoff voltage even after long-time continuous battery discharging. Under the circumstances, it would be the first step of the work to explore the elementary resistances and capacitances that affect the total cell polarization.

Shown in Fig. 2 are the typical impedance spectra for the fresh (open circle) and aged cells (open square) with a configuration of Li|1 M $LiPF_6$-EC/DEC|$LiCoO_2$, measured at an electrode potential of 4.2 V (vs Li/Li^+). The impedance spectra consist of a couple of arcs in the high and intermediate frequency range and a line inclined at a constant angle to the abscissa. The former arcs are possibly responsible for the reaction in the solid electrolyte interphase (SEI) and the interfacial charge transfer reaction combined with electrical double-layer capacitive behavior, while the latter inclined line is attributed to the solid-state lithium diffusion into the $LiCoO_2$ [6–8]. Actually, the distribution/overlapping of the time constants makes the further differentiation of the arcs difficult. Nevertheless, it seems to be reasonable to say that the arcs in the high and the intermediate frequency range are mainly attributed to the reactions in the SEI layers and the interfacial charge

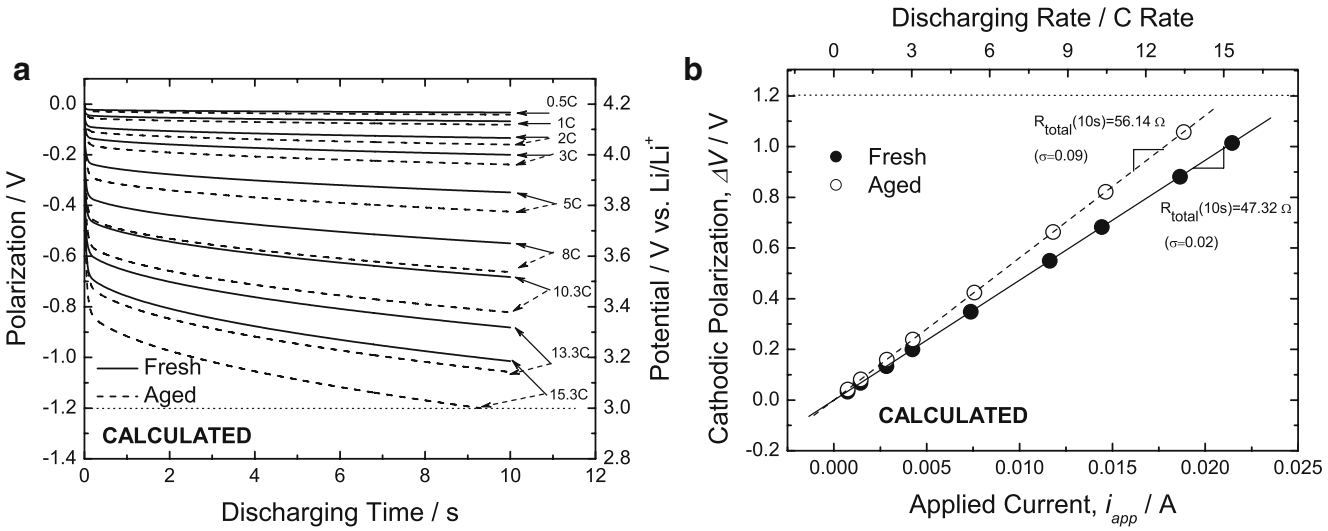

Fig. 3 **a** Calculated polarization (or potential) transients obtained from the fresh (*solid line*) and aged cell (*dotted line*) during the 10-s current pulse at a variety of discharging rates and **b** the variation of cathodic polarization at 10 s with applied current, reproduced from **a**

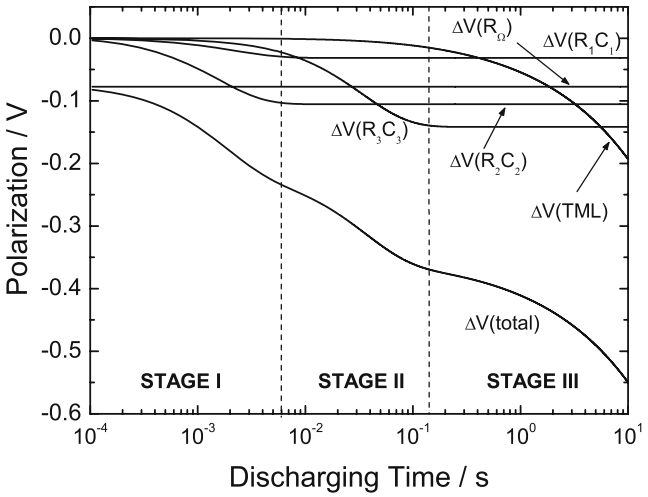

Fig. 4 Variation of elementary and total polarization of the fresh cell with logarithmic discharging time at the rate of 8*C*. Elementary polarization has been calculated for the uncompensated Ohmic resistance (R_Ω), three parallel *RC* elements (R_iC_i, i=1,2,3), and Warburg element (*TML*: transmission line)

transfer reactions combined with electrical double-layer charging, respectively, because it is agreed that the time constant for the former reactions is much less than that for the latter reactions [8].

The impedance spectra were modeled in the simplified equivalent circuit shown in the inset of Fig. 2. The first two parallel constant phase element (R-CPE) elements represent the highly depressed arcs in the high frequency range, while the third parallel R-CPE element stands for the arc in the intermediate frequency range. The values of resistance, capacitance, and the chemical diffusion coefficient of lithium into the $LiCoO_2$ were determined by using the complex nonlinear least squares (CNLS) fitting methods (the solid lines in Fig. 2 and Table 1). Because the Nyquist plot of Fig. 2 showed the clear difference in the time constants of the apparent reaction steps, phenomenological analysis of impedance spectra could be done with little doubt. Actually, the two-electrode electrochemical cells adopted in this work, however, places a limitation on exact differentiation of the time constants of the actual reaction steps of, e.g., the reactions caused by anode and cathode sides. The future work would be the further differentiation of the contribution of anode and cathode using three-electrode electrochemical cells under a variety of test conditions.

On the basis of these results, we reconstruct the equivalent circuit for the purpose of circuit simulation as follows: we regarded all the CPE components as the purely capacitive components. This leads to some discrepancy between the experimental potential transients and simulated potential transients because of the disregard of the fractional exponents of CPE in the theoretical calculation. Nevertheless, this approximation is thought to be reasonable because the discrepancy between experimental and simulated potential transients because of this approximation is just restricted to the very short time region (less than several hundreds milliseconds, as discussed later in this work) where the capacitive charging governs the reaction in the *RC* elements, and more importantly after the completion of the capacitive charging, the polarization is determined only by the resistive element. The Warburg impedance in the low frequency range was modeled on grounds of the transmission line analogy with diffusion [9]. The solid-state diffusion length was divided in twenty grids, assuming planar infinite-length diffusion, and the elementary resistance and capacitance were evaluated on the basis of the theory on the transmission line model [9, 10]. All the other parameters used for the circuit simulation are identical to those from the CNLS fittings.

Now, first by adopting the square cathodic current pulse source to the reconstructed equivalent circuit, the dc

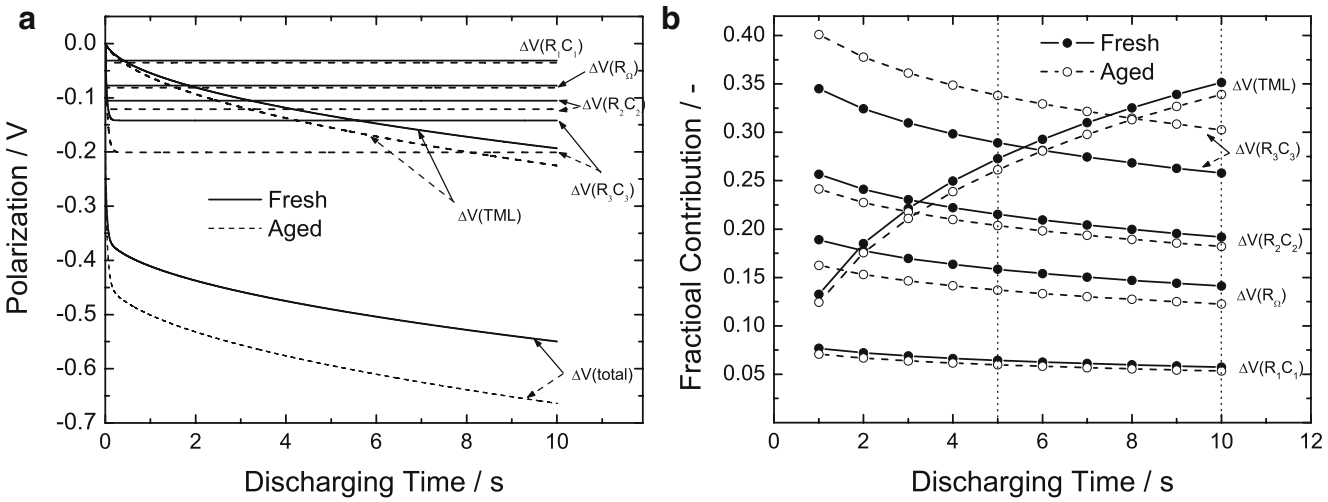

Fig. 5 **a** Variation of elementary and total polarization of the fresh (*solid line*) and aged cell (*dotted line*) with discharging time at the rate of 8*C*, and **b** dependence of fractional contribution of the elements to total polarization on discharging time, reproduced from **a**

polarization was calculated by using a simulation program with integrated circuit emphasis (SPICE) [11]. The resulting potential transients are demonstrated in Fig. 3a at a variety of discharging rates. The simulated transients are quite similar in shape to those experimentally determined (Fig. 1a). Furthermore, there is quantitative coincidence in the amount of polarization at 10 s, as shown in a cathodic polarization vs applied current plot of Fig. 3b. It is noted that the calculated polarization has a linear relationship with applied current throughout the whole discharging current range, unlike the experimental polarization where there is a deviation from the linearity at the high discharging rates above 10*C*. The difference between the experimental and simulated values of the polarization at 10 s is getting larger with increasing *C* rate, because of the additional polarization at the high current drain, which has been already discussed previously in this work.

Next, by calculating the voltage difference caused by the individual elements, one is able to estimate the contribution of individual elements to total polarization. Figure 4 exhibits the variation of elementary and total polarization with logarithmic discharging time at the rate of 8*C*. Elementary polarization has been calculated for the uncompensated Ohmic resistance (R_Ω), three parallel *RC* elements (R_iC_i, i=1,2,3), and Warburg element (*TML*: *transmission line*).

The polarization caused by the uncompensated resistance (R_Ω) remains constant throughout the discharging time, while the elementary polarization because of the R_iC_i (i= 1,2,3) elements fell in an upward convex shape, followed by a constant polarization value. The potential transients because of parallel *RC* elements can be readily explained by the fact that the charge is consumed mainly in the capacitor in the initial time range and after the completion of the charging of the capacitors, only the resistances contribute to the potential drop. The polarization because of the solid-state diffusion shows the monotonic increase in the polarization throughout the discharging time. On the other hand, it is noted that the total polarization shows three-staged behavior with two inflection points. From the results of elementary polarization transients, it is reasonable to say that the R_2C_2, R_3C_3, and transmission line elements govern the shape of the polarization transient in the stages 1, 2, and 3, respectively.

The elementary and total polarization transients, calculated for the fresh (solid line) and aged cells (dotted line), were shown in Fig. 5a. Consistent with the impedance spectra of Fig. 2, all the elementary polarizations for the aged cell are larger than the corresponding elementary polarizations for the fresh cells, indicating the increase in all the resistive elements in the cell. For the further analysis of the effect of resistive elements to total polarization, variation of the fractional contribution of all the elements to total polarization with time was reproduced from Fig. 5a, as shown in Fig. 5b. Fractional contribution gives us the information on which element significantly contributes to the total polarization in the course of the pulse-discharging process, helping us design the cell with the improved power capability.

For instance, at the 5-s discharging pulse, which corresponds to the 5-s continuous acceleration of the (hybrid) electric vehicle, the parallel R_3C_3 element makes a maximum contribution (30% for the fresh cell and 35% for the aged cell) to the total polarization. Accordingly, the surface design to reduce the interfacial charge transfer resistance, e.g., surface modification of the active material [12–14], would be the most effective way to improve the 5-s pulse capability. As for the 10-s discharging pulse, the diffusion resistance is responsible for approx. 35% of the total polarization in both the fresh cell and the aged cell. In this case, the materials design to increase the chemical diffusion coefficient of lithium through the active material, e.g., microstructural control in the bulk [15, 16], would be the first approach to improve the 10-s pulse capability.

Conclusions

In the present work, the practical method to analyze the time dependence of the elementary polarization in the course of current pulse discharging has been suggested. This includes the circuit analysis, based on the results of the electrochemical impedance spectroscopy. The contribution of the uncompensated ohmic resistance, interfacial impedance, and diffusion impedance to total cathodic polarization has been satisfactorily distinguished. Furthermore, examples to design the high-power battery have been given on grounds of the concept of fractional contribution of the elements to total polarization. The method suggested in this work gives a fast and reliable way to analyze the polarization at a variety of pulse signals and is expected to help us design the high-power battery systems.

Acknowledgments This work was supported by the Korea Research Foundation Grant funded by the Korean Government (MOEHRD; KRF-2006-331-D00713). Incidentally, this work was partially supported by a grant-in-aid for the National Core Research Center Program from the Ministry of Science and Technology and the Korea Science and Engineering Foundation (no. R15-2006-022-01001-0).

References

1. Horiba T, Maeshima T, Matsumura T, Koseki M, Arai J, Muranaka Y (2005) J Power Sources 146:107
2. Sawai K, Yamato R, Ohzuku T (2006) Electrochim Acta 51:1651
3. Chen ZH, Amine K (2006) J Electrochem Soc 153:A1221

4. Balakrishnan PG, Ramesh R, Prem Kumar T (2006) J Power Sources 155:401
5. Abraham KM, Pasquariello DM, Willstaedt EM (1998) J Electrochem Soc 145:482
6. Yoskiike N, Ayusawa M, Kondo S (1984) J Electrochem Soc 131:2600
7. Thomas MGSR, Bruce PG, Goodenough JB (1985) J Electrochem Soc 132:1521
8. Levi MD, Salitra G, Markovsky B, Teller H, Aurbach D, Heider U, Heider L (1999) J Electrochem Soc 146:1279
9. Barsoukov E, Macdonald JR (2005) Impedance spectroscopy. Wiley, Hoboken, NJ
10. Bisquert J, Garcia-Belmonte G, Fabregat-Santiago F, Roberto Bueno P (1999) J Electroanal Chem 475:152
11. Shin HC, Pyun SI (2003) Mechanisms of lithium transport through transition metal oxides and carbonaceous materials. In: Vayenas CG, Conway BE, White RE (eds) Modern aspects of electrochemistry, no. 36. Kluwer, New York, pp 255–301
12. Groult H, Nakajima T, Perrigaud L, Ohzawa Y, Yashiro H, Komaba S, Kumagai N (2005) J Fluorine Chem 126:1111
13. Takamura T, Eguchi S, Suzuki J, Omae O, Sekine K (2005) J Power Sources 146:129
14. Fu LJ, Liu H, Li C, Wu YP, Rahm E, Holze R, Wu HQ (2006) Solid State Sci 8:113
15. Deiss E, Haringer D, Novak P, Haas O (2001) Electrochim Acta 46:4185
16. Myung ST, Kumagai N, Komaba S, Chung HT (2001) Solid State Ionics 139:47